Application of the Maxwell–Stefan theory to the membrane electrolysis process. Model development and simulations

Hogendoorn, J.A.; Veen, A.J. van der; Stegen, J.H.G. van der; Kuipers, J.A.M.; Versteeg, G.F.

Published in:
Computers and Chemical Engineering

Publication date:
2001

ELSEVIER

Computers and Chemical Engineering 25 (2001) 1251–1265

Computers & Chemical Engineering

www.elsevier.com/locate/compchemeng

Application of the Maxwell–Stefan theory to the membrane electrolysis process Model development and simulations

J.A. Hogendoorn [a,b], A.J. van der Veen [a,1], J.H.G. van der Stegen [a], J.A.M. Kuipers [a,b], G.F. Versteeg [a,b,*]

[a] *AKZO-Nobel Central Research B.V., RTB department, P.O. Box 9300, 6800 SB SB Arnhem, The Netherlands*
[b] *Department of Chemical Engineering, University of Twente, P.O. Box 217, 7500 AE Enschede, The Netherlands*

Received 11 April 2000; received in revised form 1 March 2001; accepted 1 March 2001

Abstract

A model is developed which describes the mass transfer in ion-selective membranes as used in the chloralkali electrolysis process. The mass transfer model is based on the Maxwell–Stefan theory, in which the membrane charged groups are considered as one of the components in the aqueous mixture. The Maxwell–Stefan equations are re-written in such a way that the current density can be used as an input parameter in the model, which circumvents an extensive numerical iterative process in the numerical solution of the equations. Because the Maxwell–Stefan theory is in fact a force balance, and the clamping force needed to keep the membrane charged groups in its place is not taken into account, the model is basically over-dimensioned: the mole fraction of the membrane can be calculated by using the equivalent weight (EW) of the membrane or by using the equations of continuity. In this work, the latter method has been chosen. The results of the computer model were verified in several ways, which show that the computer model gives reliable results. Several exploratory simulations have been carried out for a sulfonic layer membrane and the conditions as encountered in the chloralkali electrolysis process. As there are no (reliable) Maxwell–Stefan diffusivities available for a Nafion membrane, in this trend study the diffusivities were all chosen equal at a more or less arbitrary value of 1.10^{-10} m^2 s^{-1}. Due to this, the absolute values of several performance parameters are incorrect as compared with industrial chloralkali operation (e.g. an unrealistically high current efficiency of 95.7% was found), but the model can still be used to obtain trends. For example, it is shown that the thickness of the membrane hardly increases the current efficiency (CE), however, the required potential drop proportionally increases with thickness. The pH rapidly increases to values greater than 12 just inside the membrane at the anolyte side. Moreover, for different values of the pH in the anolyte, the pH profiles inside the membrane nearly coincide with each other. A change in the anolyte strength does not have a significant effect on the performance of the membrane. At low values of the current density, a high value of the current efficiency is found. However, this is not due to a low OH^- counter flux, but to the simultaneous transport of OH^- and Cl^- towards the catholyte.

Keywords: Maxwell–Stefan theory; Membrane electrolysis process; Mass transfer

Nomenclature

A	matrix with non-idealities, transference numbers and diffusivities (mol m^{-1} s^{-1})
$A_{i,j}$	mass transfer parameter (follows from $(B^{n*})^{-1}(\Xi)$) (mol m^{-1} s^{-1})
B^{n*}	matrix with diffusivities (s m mol^{-1})

* Corresponding author. Tel.: +31-53-4894337; fax: +31-53-4894774.
E-mail address: g.f.versteeg@ct.utwente.nl (G.F. Versteeg).
[1] Present address: Shell Moerdijk, The Netherlands.

0098-1354/01/$ - see front matter
PII: S0098-1354(01)00697-4

$B_{i,j}$	coefficient with electrical and mass transfer parameters (s m mol^{-1})
$B^n_{i,j}$	transport coefficient (s m mol^{-1})
$B^n_{i,j}$*	modified transport coefficient (s m mol^{-1})
CE	current efficiency (−)
CD	current density (A m^{-2})
c_i	concentration of component i (mol m^{-3})
c_T	total concentration (mol m^{-3})
d_i	driving force of component i (J m^{-4})
$Đ_{i,j}$	binary Maxwell–Stefan diffusivity (m^2 s^{-1})
F	Faraday constant (96487 C mol^{-1}) Coulomb mol^{-1})
I	current density (Coulomb m^2 s^{-1})
J^n_i	molar diffusive flux with respect to component n (mol m^{-2} s^{-1})
$K_{i,j}$	friction coefficient (Js m^{-5})
$L^n_{i,j}$	inverted transport coefficient (follows from the inverse of (M^n)) (m^5 J s^{-1})
$M_{i,j}$	modified transport coefficient (follows from (K)) (J s m^{-5})
$M^n_{i,j}$	modified transport coefficient ((M) without the nth row and column) (J s m^{-5})
N_i	molar flux of component i (mol m^{-2} s^{-1})
n	total number of components (−)
P	pressure (Pa)
R	universal gas constant (8.314413 J mol^{-1} K^{-1}) (J mol^{-1} K^{-1})
T	temperature (K)
t^n_i	transference number of component i with respect to component n (−)
v_i	velocity of component i (m s^{-1})
x_i	mole fraction of component i (−)
$\boldsymbol{Z}_i$	electrical coefficient (1 m^{-1})
Z^*_i	electrical coefficient (s m mol^{-1})
$Z^{\#}_{i,j}$	electrical coefficient (Coulomb sm^{-1})
z_i	ionic charge of component i (−)

Greek

α_i	mass transfer parameter (follows from $[B^n*]^{-1}(Z*)$) (mol Coulomb m^{-2})
$\beta i,j$	mass transfer parameter (follows from $[B^n*][Z^{\#}]$) (mol m^{-2} s^{-1})
$\Gamma_{i,j}$	thermodynamic factor (−)
γ_i	activity coefficient of component i (−)
$\delta_{i,j}$	Kronecker-delta ($\delta_{i,j}=1$ for $i=j$ and $\delta_{i,j}=0$ for $i\neq j$) (−)
φ	electrical potential (mol m^{-3})
κ	conductivity (1 Ω m^{-1})
μ_i	electrochemical potential of component i (mol m^{-3})
μ°_i	chemical potential of component i in the reference state (mol m^{-3})
μ^{chemical}_i	chemical potential of component i (mol m^{-3})
$\Xi_{i,j}$	factor consisting of transport and thermodynamic factors (−)
$\Xi^*_{i,j}$	factor consisting of transport and thermodynamic factors (−)

Sub/superscript

i	component index or index of vector/matrix
j	component index or index of vector/matrix
n	nth component

Mathematical

( )	vector
[ ]	matrix
[ ]$^{-1}$	inverse of a square matrix
∇	gradient
Bold	vectorial quantity
(∇x)	divergence of a vector field

1. Introduction

Chlorine is one of the world's most important chemicals and is used not only to produce (consumer) end products, but also to produce a large amount of chlorinated intermediate products as applied in e.g. organic substitution reactions. Chlorine is obtained via the chloralkali electrolysis process, which uses NaCl as basic material. The main reaction of the chloralkali electrolysis is:

$$2NaCl + 2H_2O \rightarrow Cl_2 + 2NaOH + H_2$$

In practice three different types of electrolysis cells are used; the mercury cell, the diaphragm cell, and the membrane cell. The present study restricts the attention to the membrane electrolysis process. In this process, the cell consists of a cathode and an anode compartment divided by a cation-selective membrane (see Fig. 1). The anode compartment is fed with a brine solution and at the anode gaseous chlorine is formed. The cathode compartment is fed with water and at the cathode gaseous hydrogen and hydroxyl ions are produced. The sodium ions diffuse and migrate through the ion-selective membrane from the anode to the cathode compartment. Combined with the hydroxyl ions, sodium leaves the membrane cell as sodium hydroxide. Although this process is used industrially on a large scale, only a very limited number of studies have dealt with the fundamental description and basic understanding of the mass transfer process in the ion-selective membrane. To our knowledge, the results of the (fundamental) mass transfer models have never been compared with the experimental results as obtained for industrially used multi-layer membranes for the conditions as used in industry.

The cation membranes in the chloralkali electrolysis frequently consists of two or three polymeric layers: one with sulfonic groups (sulfonic layer) and one or two with carboxylic groups (carboxylic layers). These cation selective membranes absorb the ions selectively when contacted with an electrolyte solution (often referred to as Donnan exclusion). The membrane rejects equally charged ions (co-ions), while oppositely charged ions (counter-ions) are preferentially absorbed. The various layers in the membrane will differ with respect to the sorption properties of the ions and water, resulting in concentration discontinuities at the various phase transitions (see for example Fig. 2). Also the transport properties of the ions in the different membrane layers will vary. Both aspects, the sorption of the ions at the various interfaces and the transport of the ions in the membrane layers, have to be incorporated in a mass transfer model in order to obtain a reliable simulation model. Furthermore, the mass transfer model itself should, of course, represent the actual mass transfer phenomena occurring in the membrane in a realistic way. The sorption of ions at the various membrane interfaces is usually described by the Donnan equilibria. However, this is a very simplified representation of reality. van der Stegen, van der Veen, Weerdenburg, Hogendoorn and Versteeg (1999a) has shown that the equilibria at the liquid–membrane interfaces can be more accurately be described using a modified Pitzer equilibrium model.

In the present contribution, a mass transfer model based on the Maxwelll–Stefan theory will be developed in order to describe the mass transfer through ion-selective layers. For the description of the equilibria at the liquid–membrane interfaces as required in the mass transfer model the modified Pitzer model as previously developed by van der Stegen et al. (1999a) is used.

2. Application of the Maxwell–Stefan theory to the membrane electrolysis process

2.1. Introduction

In the present model formulation the charged groups of the ion-selective membranes are considered as an

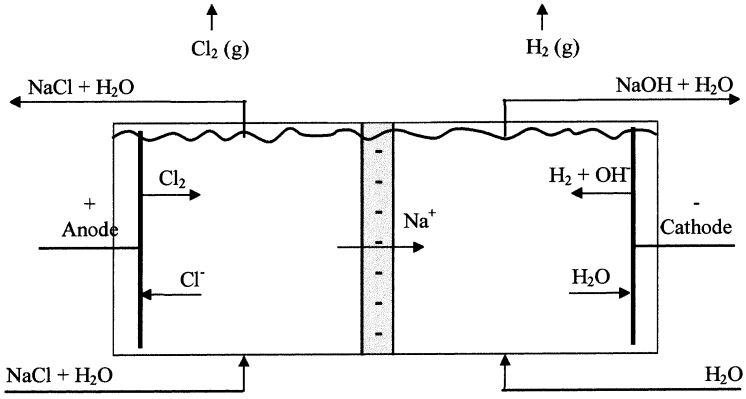

Fig. 1. Schematic representation of the chloralkali process in a membrane cell.

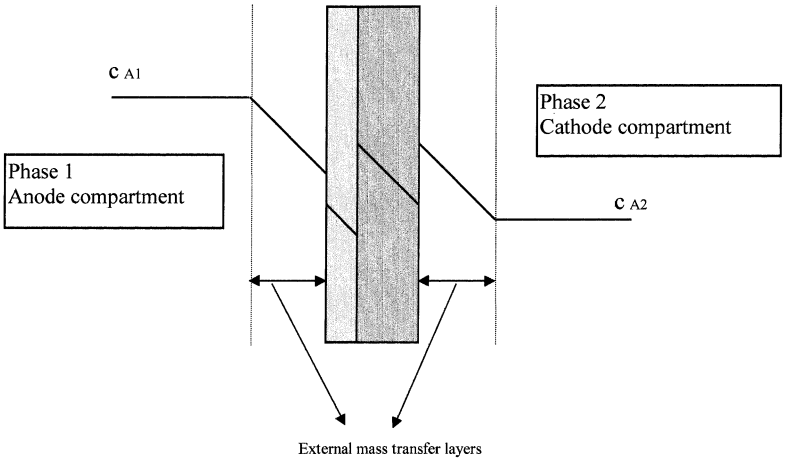

Fig. 2. Schematic representation of a possible concentration profile of a component A in a two-layer membrane. For simplicity reasons straight concentration profiles are assumed. Note the concentration discontinuities at the various interfaces.

individual component present in the system and, therefore, also as a component in the Maxwell–Stefan equations. In this way the description is similar to the treatment of the transport in porous media as described with the Dusty Gas Model (Mason & Malinauskas, 1983). In the present contribution the Maxwell–Stefan equations are re-written in such a way that the potential gradient is eliminated from the model equations and replaced by the current density. This has been done because in the electrolysis industry the current density is a control parameter, and should therefore preferably be used as an input parameter in the model. Moreover, by using the current density in the model equations instead of the potential gradient, a cumbersome and time-consuming iterative procedure of adjusting the potential drop over the membrane until the desired current density is reached is avoided.

In this section, the transport equations based on the Maxwell–Stefan theory are given which are required for the description of the transport in the membrane electrolysis cell. As mentioned before, in the model it is assumed that the charged groups of the membrane can be regarded as one of the components in the aqueous electrolyte solution. The membrane charged groups are kept in place by some arbitrary external, clamping force.

2.2. Degrees of freedom

Before discussing the mass transfer model in detail first a discussion about the degrees of freedom is required. If a mass transport model is applied to a non-ionic solution, then there are basically $(n-1)$ independent flux equations (continuity) and one equation originating from the Gibbs–Duhem condition that states that

$$\sum_{i=1}^{n} x_i = 1 \quad i = n \tag{1}$$

For an electrolyte solution the number of independent flux equations decreases to $(n-2)$ as one additional equation has to be fulfilled dictated by the Gibbs–Duhem condition:

$$\sum_{i=1}^{n} z_i x_i = 0 \quad i = n-1 \tag{2}$$

In the present model, the charged groups of the membrane are considered as 'ordinary' ions. This means that the mass transfer model should basically comprise of $(n-2)$ flux equations complemented by Eqs. (1) and (2). The concentration (or mole fraction) of the charged groups in the membrane and the mole fractions of all other components can now be calculated by applying the mass transport model and appropriate boundary conditions.

On the other hand, the concentration of the membrane, in this case the concentration of the fixed charged groups in the membrane, is also known throughout the membrane because it is an a priori known membrane property determined by the so-called equivalent weight. Therefore, the membrane process should actually be defined by $(n-3)$ independent mass transport equations combined with Eqs. (1) and (2) and an additional equation that describes the mole fraction of the ionic groups in the membrane. However, rearrangement of the set of mass transfer equations to include this demand and arrive at $(n-3)$ independent flux equations (in a similar way the demands imposed by Eqs. (1) and (2) can be included in the mass transport equations so that $(n-2)$ independent flux equations remain) is impossible. The reason for this is that the number of equations exceeds the number of unknowns. The membrane concentration can be calculated with the mass transfer model on one hand (using

$(n-2)$ independent flux equations combined with Eqs. (1) and (2)), but at the same time it can be regarded as a membrane property and hence the mole fraction can also be calculated from that (so without any mass transfer model). This makes the problem over-specified. If it is kept in mind that the Maxwell–Stefan theory is in fact a force balance, this over-specification can be explained, in the mass transport model no clamping force for the membrane groups is inserted, which is actually required to keep the membrane at its position during the transport process. If this force was introduced, there would be one extra degree of freedom and the system would be described mathematically correct. However, it seems not useful to introduce such a clamping force because it would simply be a fitted parameter. Therefore, it was omitted from the model, which results in an over-specified problem from a fundamental point of view. Based on this complication two correctional approaches can be followed.

1. Solving $(n-2)$ equations of continuity. The mole fractions of the other two components follow from the summation of the mole fractions (Eq. (1)) and the condition of electroneutrality (Eq. (2)).
2. Solving the equation of continuity in combination with the specified membrane concentration. The number of continuity equations of continuity is in this case $n-3$. The mole fractions of the other three components follow from the summation of the mole fractions (Eq. (1)), the condition of electroneutrality (Eq. (2)) and from the specified membrane concentrations.

If the first method is followed, then the molar fluxes of all components turn out to be constant in the steady state (i.e. the molar fluxes are no function of position in the mass transfer layer). However, the calculated membrane concentration does not exactly coincide with the independently determined and a priori known membrane concentration. On the other hand, if the second approach is followed this discrepancy is avoided because this concentration has been imposed. However, in this case the molar flux of one component is not constant in the steady state. It is obvious that a choice has to be made between.

1. Demanding that all components have a constant molar flux in the steady state, which implies that the membrane concentration cannot be specified. Preliminary model calculations (the complete model is treated in subsequent sections) have shown that in this case deviations between the experimental membrane concentration and the calculated membrane concentration up to a few percent can occur.
2. Specifying the membrane concentration. In this case the molar flux of one component is not constant. Scouting calculations with the model (presented in Section 2.3) have shown that for this case variations in the molar flux of this component up to 30% can occur.

For the present study the first approach was selected. A fundamental principle of mass transfer processes is that the molar fluxes of all components are constant in the steady state, so that no accumulation in the system occurs.

2.3. Derivation of the transport equations for the mass transfer in an electrochemical system

The Maxwell–Stefan theory is a steady state force balance in which the total sum of the driving forces acting on a molecule of a certain component are equal to the friction forces acting on the molecule. In multicomponent systems all interactions (frictions) between a molecule with other types of molecules present in the solution are taken into account. For each component i in a mixture a Maxwell–Stefan equation can be formulated, which can be represented as (Taylor & Krishna, 1993):

$$c_i \nabla_{T,P} \mu_i = RT \sum_{j=1}^{n} \frac{c_i c_j}{c_T Đ_{i,j}} (v_j - v_i) = RT \sum_{j=1}^{n} \frac{x_i N_j - x_j N_i}{Đ_{i,j}} \tag{3}$$

The left hand side of Eq. (3) contains all driving forces of the mass transfer process, the right hand side contains the interactions between a component i with all other components present in the system. The friction between the various components is lumped in the various Maxwell–Stefan diffusivities, $Đ_{i,j}$, which are a measure of the interaction between component i and j.

In Eq. (3) the electrochemical potential is defined as:

$$\mu_i = \mu_i^{\text{chemical}} + z_i F \varphi = \mu_i^0 + RT \ln(x_i \gamma_i) + z_i F \varphi \tag{4}$$

For the development of the present model the main assumptions are.

- No convective transport due to pressure differences over the membrane occurs. However, in practice, a small pressure difference over the membrane (± 0.1 bar) is applied in order to assure that the membrane is pressed against the anode. Preliminary estimations, however, have shown that the pressure difference causes a negligible contribution to the total driving force compared with those of the concentration and potential gradient (Taylor & Krishna, 1993).
- The transport process in the membrane is isothermal. The assumption that the mass transfer process is isothermal, makes it superfluous to implement and simultaneously solve the energy balance in the mass transport model. This assumption is allowed because no reactions, and, therefore, no heat consumption or evolution takes place inside the membrane. Moreover, the heat generated due to Ohmic resistance (calculated according to the method described in Taylor & Krishna, 1993) was estimated to be negligible: for typical conditions of the chloralkali electrol-

ysis process the temperature rise in the membrane was less than 0.2 K.

As a result of the above assumptions the mass transfer rate is determined by two gradients, a gradient in the activity ($x_i\gamma_i$) and a gradient in the electrical potential. It is possible to combine these gradients into one overall gradient of the mole fraction. In this way, the driving force of the mass transfer process can be expressed as a function of one set of variables, the mole fractions of the components present in the mixture. Solving the transport equations for a specified current density results in this case in the calculation of the mole fraction profile and the molar fluxes. With these results the electrical potential profile in the membrane can then be obtained. The exact derivation of the resulting transport equations has been given in Appendix A. The mass transfer process in a mixture consisting of n components (including the solvent as the $(n-1)$th and the membrane charged groups as the nth component) can be described with the following equations (in matrix notation).

- $n-2$ Independent Maxwell–Stefan equations for components 1 to $n-2$:

$$(N) = [A](\nabla x) - [\beta]x \tag{5}$$

  in which N is the matrix with the $(n-2)$ fluxes with respect to the (in time and space stationary) membrane (see Appendix A).
- Two supplementary equations for component $n-1$ and n:

$$\sum_{i=1}^{n} x_i = 1 \quad i = n \tag{1}$$

$$\sum_{i=1}^{n} z_i x_i = 0 \quad i = n-1 \tag{2}$$

For steady state operation, the equation of continuity holds:

$$\left(\frac{\mathrm{d}N_i}{\mathrm{d}z}\right) = 0 \quad i = 1, 2, \ldots, n \tag{6}$$

and, therefore, the molar fluxes are not functions of position in the membrane.

The set of Eqs. (1), (2), (5) and (6) are second order differential equations. So, for each component two boundary conditions are required in order to solve the set of equations uniquely.

2.3.1. Boundary conditions

It is assumed that at the phase transition between liquid and membrane at both the anolyte and catholyte side locally equilibrium holds (see Fig. 2, note that this does not implicate that no mass transfer resistance can be present in the liquid (or membrane)). For an ion-selective material these equilibria are often described using Donnan-equilibrium expressions. In a previous paper, van der Stegen et al. (1999a) has shown that these equilibria can more extensively and accurately be described by a modified Pitzer equilibrium model. This model has been used to predict the composition just inside the membrane at $x = 0$ and $x = L$ for a given composition just outside the membrane (i.e. catholyte and anolyte side, see Fig. 2 for a schematic representation). This way the boundary conditions for the mass transfer model could be determined.

2.3.2. Numerical technique

In the present study, a numerical technique was used which enables the calculation of the non-steady state version of Eq. (6). The resulting set of partial differential equations was solved with the help of a finite difference technique as proposed by Baker and Oliphant (Taylor, Hoefsloot & Kuipers, 1995). The main reason for solving the unsteady state version of Eq. (6) in combination with Eqs. (1), (2) and (5) is that the numerical solution method is more stable and less sensitive to the initial guesses. For this unsteady state calculation procedure initial concentration profiles are required, which were arbitrarily chosen as straight concentration profiles in each mass transfer layer inside the membrane. The calculation procedure was continued until the concentration profiles became time-independent, which meant that a steady state situation was obtained.

It is emphasized that in the presently derived form of the Maxwell–Stefan equations, the current density is an input parameter, and not a parameter which can only be determined after the complete mass transfer problem is solved. This means that with the present formulation a cumbersome, time consuming, iterative procedure is avoided.

2.4. Computer model

Based on the theory presented, a mathematical model has been developed and solved numerically. As already mentioned in the previous section an implicit discretization technique according to the scheme of Baker and Oliphant was used for the discretization of the partial differential equations (see Taylor et al., 1995).

The computer model contains the following elements.

1. The number of components can be chosen freely.
2. The number of mass transfer layers can be chosen freely including external mass transfer resistances. For each mass transfer layer, the model needs a specific set of data with the physical and thermodynamic properties and the material properties (for the membrane phases) of that layer. The required data can be inserted in the computer model. The required physical parameters can be implemented as a function of composition, temperature and pressure.

3. The computer model includes the modified Pitzer model for the determination of the activity coefficients in the membrane and the equilibria at the various interfaces (see van der Stegen et al., 1999a).

For any arbitrary initial profile, the computer model calculates the steady state of the mass transfer process and returns the mole fraction profiles and molar fluxes of the components present in the system as a function of position. Further, also the electrical potential profile is calculated using Eq. (A.13) (see Appendix A).

2.5. Verification of the algorithm of the computer model

The algorithm of the computer model was extensively verified; i.e. the results of the model were compared with the analytical results for various asymptotic situations. In another paper (van der Stegen van der Veen, Weerdenburg, Hogendoorn & Versteeg, 1999b), the model results are fitted to experimental results of a chloralkali electrolysis process to obtain a set of Maxwell–Stefan diffusivities for this process and therewith be able to predict the performance of the process at various conditions.

Firstly, for both a single layer and a multi-layer membrane (with arbitrarily chosen properties), the condition of the continuity of the fluxes was verified. The fluxes were constant with less than 10^{-4}% difference at the various positions in the membrane (even at the interfaces where due to the liquid–membrane or membrane–membrane transition a discontinuity in the mole fractions occurs, these equilibria are described by the modified Pitzer model as developed by van der Stegen et al. (1999a)). Secondly, for a one layer membrane the model output (mole fraction profile and potential profile) was substituted in the original Maxwell–Stefan equations (relation 1), which yielded a good agreement. Thirdly, a one layer membrane was fictively subdivided in three different separate layers, all having identical properties. The model results for the one layer model were identical to that of the three layer model. Fourthly, for a very diluted 1:1 electrolyte solution without the presence of a membrane or potential difference, the model results were compared with Fick's law (which is valid for these conditions), which also yielded excellent agreement. Fifthly, for a very diluted electrolyte solution containing no membrane and 1 type of positive ions and two types of negative ions (e.g. a NaOH/NaCl aqueous mixture), the model output was compared with the predictions of the Nernst–Planck model for a current density of $CD = 0$ A m^{-2} and $CD = 1$ A m^{-2}. For these conditions, the Nernst–Planck model yields an approximate solution for the Maxwell–Stefan equations. Also this comparison showed a good agreement. Furthermore, several asymptotic situations have been simulated, to see if the model behaves according to the expectations. For example, in one of the simulations carried out a three layer membrane was chosen, in which the diffusivities in the second layer were chosen very large. Indeed, the model results indicated that the mole fraction and potential profile were nearly flat (i.e. constant) in the second layer.

From the test results, it was concluded that the outcome of the computer model satisfies the original model equations. Thus it can be used reliably to simulate the mass transfer process according to the Maxwell–Stefan theory in a membrane used in the chloralkali electrolysis process.

Table 1
The Maxwell–Stefan diffusivities and the selection which has been incorporated in the model calculations

Diffusivity	Incorporated in the calculations
$Đ_{Cl-w}$	Yes
$Đ_{OH-w}$	Yes
$Đ_{Na+w}$	Yes
$Đ_{m,w}$	Yes
$Đ_{Cl-OH-}$	No
$Đ_{Cl-Na+}$	No
$Đ_{Cl-m}$	No
$Đ_{OH-Na+}$	No
$Đ_{OH-m}$	No
$Đ_{Na+m}$	Yes

3. Model simulations

In this section, the results of the model simulations will be presented which demonstrate the influence of process parameters on the performance of the chloralkali electrolysis process. This influence on the performance is simulated for a relatively simple configuration consisting of a single-layer cation-selective sulfonic membrane for conditions as encountered in the chloralkali electrolysis process. The present study gives some numerical examples to show the capabilities of the model without extensive comparison or fitting to experimental chloralkali electrolysis data, this is done in another study (van der Stegen et al., 1999b). Because no complete set of Maxwell–Stefan diffusivities for the various components is available for these ion-selective sulfonic membranes, and because the present study is not aimed at an extensive comparison with experimental data a reduced set of Maxwell–Stefan diffusivities was used in the simulations. In Table 1 all Maxwell–Stefan diffusivities as encountered in the chloralkali industry are summarized. To determine the set of relevant Maxwell–Stefan diffusivities, initially, all these diffusivities were given an equal value of 1.10^{-10} m^2 s^{-1}. This value was derived from the approximate

Table 2
Base case conditions and calculated performance of the sulfonic membrane for these conditions[a]

Membrane and process conditions		
NaCl in anolyte	180 g dm^{-3}	
NaOH in catholyte	23 wt.%	
pH anolyte	5	
Thickness sulfonic membrane	61.8×10^{-6} m	
$EW_{membrane}$	1100 g mol^{-1}	
Current density (CD)	2000 A m^{-2}	
Calculated mole fractions (−)	Anolyte	Catholyte
Cl^-	0.055	2.03×10^{-5}
Na^+	0.055	0.106
OH^-	0	0.106
H_2O	0.89	0.79
Calculated data		
Flux Na^+ (mol m^{-2} s^{-1})	1.98×10^{-2}	
Flux Cl^- (mol m^{-2} s^{-1})	4.40×10^{-5}	
Flux OH^- (mol m^{-2} s^{-1})	-9.36×10^{-5}	
Flux H_2O (mol m^{-2} s^{-1})	8.45×10^{-2}	
Water transport number	4.08 mol F^{-1}	
Current efficiency (CE)	95.7%	
Potential drop	0.149 V	

[a] A positive flux resembles a flux from the anode to the cathode side.

value of Fick's law diffusivities in aqueous solutions and applying a correction for the tortuosity and porosity of the membrane. With these values and the complete set of Maxwell–Stefan diffusivities preliminary simulations were carried out in which one of the diffusivities was changed with several orders of magnitude without changing the other ones. If the change did not seriously affect the simulation results, the specific diffusivity was regarded as 'unimportant'. On the other hand, if a change of a specific diffusivity led to a considerable change in the simulation results, the diffusivity was regarded as 'important'. In Table 1 the selection of Maxwell–Stefan diffusivities which has been taken into account is denoted with 'yes', and constitutes of the Maxwell–Stefan diffusivities of the ions with water and the Maxwell–Stefan diffusivity of Na^+ with the membrane. Because the membrane is cation selective the uptake of Cl^- and OH^- will be relatively small, and, therefore, the interaction of these ions with other ions in the membrane is small and shown to be negligible according to some preliminary calculations (not shown here). The value of the selected diffusivities was chosen at a value of 1.10^{-10} m^2 s^{-1}. The other diffusivities were given a value 1.10^{-4} m^2 s^{-1} thereby excluding any influence by them. Of course, the present selection of the Maxwell–Stefan diffusivities and the values of these diffusivities does not pretend to be complete or correct, so only a qualitative impression of the behavior of such a sulfonic membrane can be obtained. Nevertheless, interesting phenomena can be observed.

The sulfonic membrane chosen has the same properties as the sulfonic layer of the Nafion DuPont membrane with an equivalent weight of 1.1 kg mol^{-1}. In a previous paper (van der Stegen et al., 1999a) developed a modified Pitzer equilibrium model to describe the equilibria between a liquid and an ion-selective membrane. In the present mass transport model equilibrium is assumed at the membrane–liquid interfaces. This means that the modified Pitzer model can be used to predict the concentrations of various species just inside the membrane for a given composition of the liquid just outside the membrane. In the mass transfer model it is further assumed that the mass transfer resistance from the bulk towards the membrane is negligible, so the composition at the liquid side of the membrane–liquid interfaces is equal to the anode and cathode composition, respectively. This means that the overall resistance against mass transfer is located in the membrane itself.

The influence of the thickness of the membrane (30–75 μm), the anolyte concentration (150–220 g l^{-1}) the current density (500–2500 A m^{-2}) and the pH in the anolyte compartment (Eqs. (1)–(6)), respectively, were studied by varying these parameters around a base case. The conditions of the base case and the corresponding simulated performance are given in Table 2. As can be seen in Table 2 the current efficiency is much higher than encountered in industrial chloralkali operation (95.7%). This is due to the fact that all diffusivities were chosen equal and the value of the diffusivities was more or less chosen arbitrarily at a value of 1.10^{-10} m^2 s^{-1}. This means that the absolute values of the performance parameters (e.g. potential drop and current efficiencies) are not directly comparable to values obtained during industrial operation, but the model can still be used to predict several trends in the aforementioned parameters.

In Fig. 3 the influence of the thickness of the membrane is given. As it can be seen the current efficiency, which is defined as the fraction of the current transported by Na^+ ions, slightly increases ($\pm$0.5%) with the thickness of the membrane. However, the potential drop over the membrane increases more or less proportionally with the thickness resulting in a proportional larger power consumption and only a small increase in current efficiency. This indicates that merely increasing the thickness of the membrane does hardly improve on the selectivity but only increases the resistance against mass transport and therewith leads to a higher potential drop. The water transport number, which is defined as the number of moles of water transported per mole of Na^+ transported, remains nearly identical at a value of 4.1 and is therefore not shown in Fig. 3. If the pH profile inside the membrane is studied it is remarkable that directly inside the membrane at the anolyte side, the pH increase rapidly to values above 7 (see Fig. 4). In Fig. 4 also the pH profile in the membrane is shown

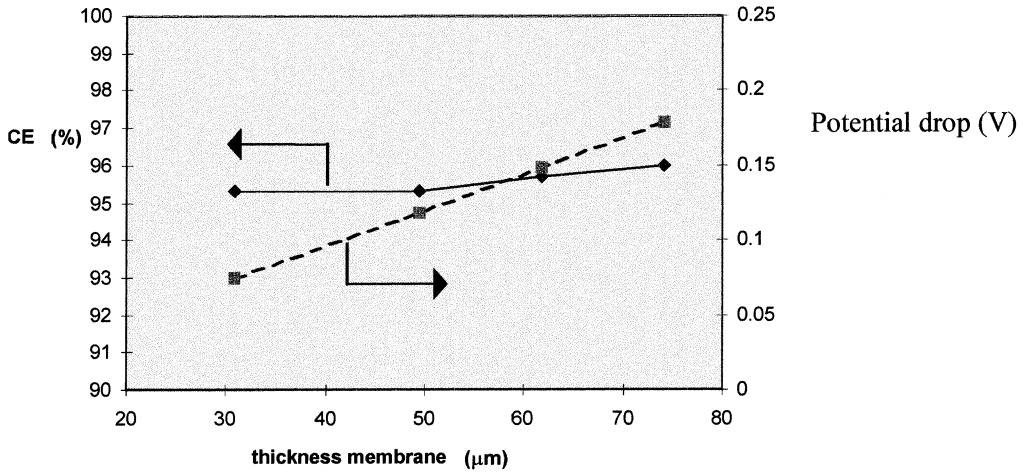

Fig. 3. Influence of the membrane thickness on the current efficiency and the potential drop across the membrane.

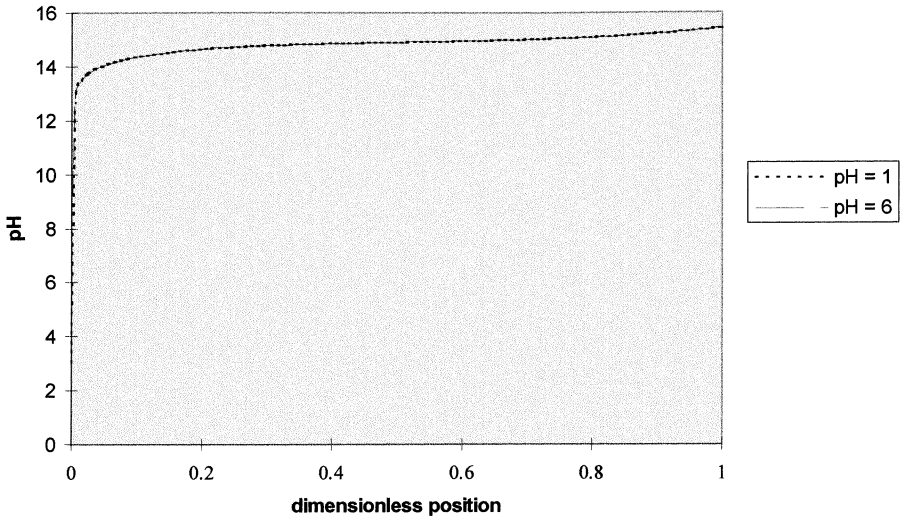

Fig. 4. Influence of pH in the anolyte on the pH profiles inside the membrane. Note that the lines for different pH's practically coincide. The dimensionless position of zero represents the anolyte side while one represents the catholyte side.

if the pH in the anolyte is changed from 6 to 1. Apart from the pH profiles directly at the anolyte side, the pH profiles inside the membrane nearly completely coincide. Also the current efficiency and potential drop over the membrane did not show a noticeable change as compared with the base case. If the anolyte strength is changed (Fig. 5), this also does not have a large influence on the current efficiency and the potential drop (potential drop is not shown but remains practically constant). Contrary, the water transport number decreases as the anolyte strength increases. This is mainly due to the fact that at higher anolyte strengths the sorption of water in the membrane decreases (see van der Stegen et al., 1999a) and therewith it affects the mole fraction profiles and consequently the fluxes. As the current density increases, the current efficiency first decreases substantially, whereafter it increases slightly again (Fig. 6). The reason for this is that at low current densities the flux of OH^- and Cl^- are of the same order of magnitude but opposite in direction. The flux of OH^- causes a current; however, the simultaneous transport of Na^+ and Cl^- in the same direction does not. Due to the simultaneous transport of Cl^-, the flux of Na^+ should be larger than in the absence of this Cl^- flux in order to meet the imposed current density. By definition of the current efficiency this leads to a higher current efficiency at an imposed current density. At higher current densities the flux of Cl^- does decrease, because the driving force for diffusion-driven transport remains constant, while the oppositely directed driving force for potential-driven transport strongly increases and therewith inhibits Cl^- transport towards the cathode. This means that at high current densities the total current is for the major part determined by the sum of fluxes of both OH^- and Na^+. In industry the current efficiency is mostly used in terms of loss of

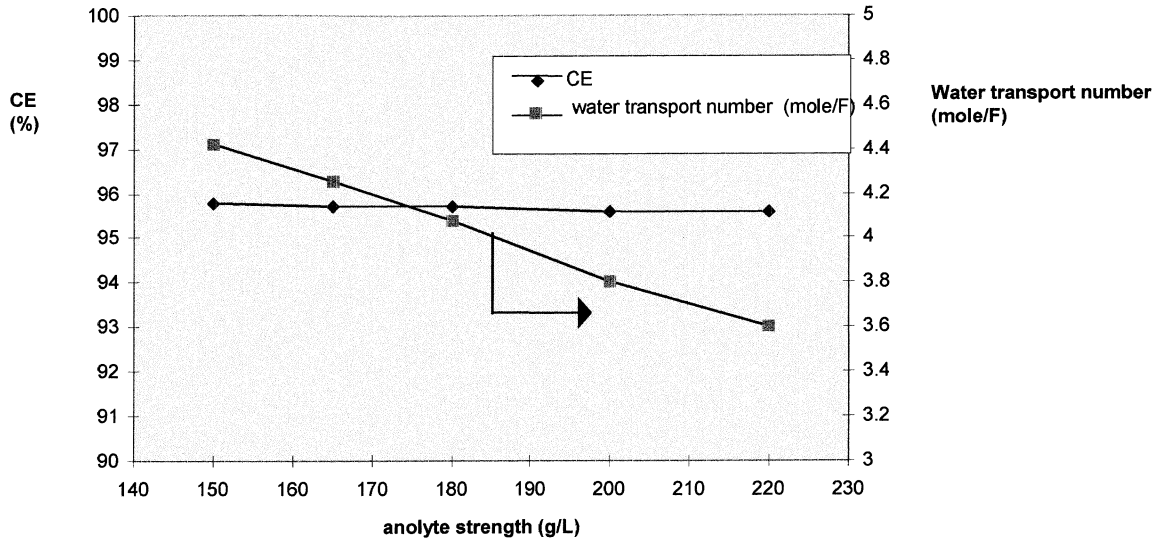

Fig. 5. Influence of the anolyte strength on the current efficiency (%) and the water transport number (mol F^{-1}).

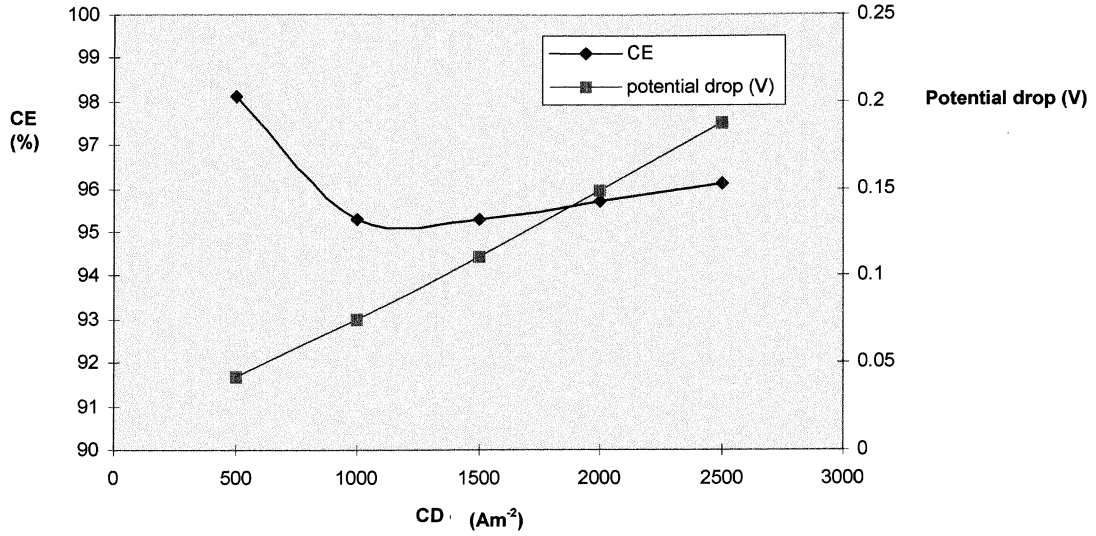

Fig. 6. Influence of the current density on the current efficiency and the potential drop across the membrane.

current due to the counter transport of OH^-. However, this example illustrates that at low current densities this rule-of-thumb definition of the current efficiency can give misleading results, although the current efficiencies calculated for low current densities seem attractively high, this is due to the definition of the current density and is at the expense of contamination of the catholyte with Cl^-. As it can be expected the potential drop across the membrane is proportionally dependent on the current density (Fig. 6).

4. Conclusions

A model has been developed which describes the mass transfer in ion-selective membranes as used in the chloralkali electrolysis process. The mass transfer model is based on the Maxwell–Stefan theory, in which the membrane charged groups were considered as one of the components in the aqueous mixture. The Maxwell–Stefan equations were re-written in such a way that the current density can be used as an input parameter in the model, which circumvents an extensive numerical iterative process in the numerical solution of the equations. Due to the fact that the Maxwell–Stefan theory is in fact a force balance, and the clamping force needed to keep the membrane charged groups in its place is not taken into account, the model is basically over-specified, the mole fraction of the membrane can be calculated by using the equivalent weight (EW) of the membrane or by using the equations of continuity. The model itself is able to predict the mole fraction of

the membrane charged groups using the equations of continuity, but this fraction can also be calculated a priori because it is a membrane property determined by the equivalent weight. It was decided not to use the equation that gives the membrane mole fraction based on the equivalent weight, but use the equation of continuity instead. This yielded only a few percent difference between the two differently calculated membrane mole fractions. The results of the computer model were verified in several ways, which showed that the computer model gives reliable results. Several exploratory simulations have been carried out for a sulfonic layer membrane and the conditions as encountered in the chloralkali electrolysis process. In the calculations a selection of the Maxwell–Stefan diffusivities was used, the selection being based on a sensitivity analysis. Because in literature no accurate Maxwell–Stefan diffusivities are available for ion-selective membranes (or other systems) the selected diffusivities were chosen equal in these exploratory calculations. Therefore, the absolute values of the various performance parameters are incorrect as compared with industrial operation (e.g. current efficiency and potential drop), but the model can be used to predict trends in these parameters with a change in operating conditions. It was shown that the thickness of the membrane hardly increases the current efficiency, however, the required potential drop proportionally increases with it. The pH rapidly increases to values >12 just inside the membrane at the anolyte side. Moreover, for different values of the pH in the anolyte, the pH profiles inside the membrane nearly coincide. A change in the anolyte strength does not seem to have a significant effect on the performance of the membrane. A low current density shows a high current efficiency, but this is due to an artifact, because it is not caused by a desired low OH^- counter flux but by the undesired transport of Cl^- towards the catholyte. It is clear that the model needs a reliable input for the Maxwell–Stefan diffusivities before it can be used to reliably simulate the performance of an industrially used membrane and applications in development and design. In another paper, these diffusivities have been be determined for the industrially used Nafion membrane of DuPont (van der Stegen et al., 1999b).

Appendix A. Development of the mass transfer model

A.1. Introduction

In this appendix the complete mass transfer model for an electrochemical system will be developed. The fundamentals of this model are constituted by the mass transport equations, which describe the mass transfer in an electrochemical system. These equations are derived in subsection A.2. For the complete description of the mass transfer in an electrochemical system a number of additional equations should be added to the mass transport equations. In subsection equation, A1.3 the complete model is given which includes all relevant equations.

A.2. Derivation of the mass transport equations

Starting point for the derivation of the set of mass transport equations is the Maxwell–Stefan equation for component i[2]:

$$c_i \nabla_{T,P}\mu_i = RT\sum_{j=1}^{n}\frac{c_i c_j}{c_T \mathcal{D}_{i,j}}(v_j - v_i) = RT\sum_{j=1}^{n}\frac{x_i N_j - x_j N_i}{\mathcal{D}_{i,j}} \quad (A.1)$$

The driving force for the mass transport is the electrochemical potential gradient $\nabla\mu_i$, in which the electrochemical potential μ_i is defined as follows:

$$\mu_i = \mu_i^{\text{chemical}} + z_i F\varphi = \mu_i^{\circ} + RT\ln(x_i\gamma_i) + z_i F\varphi \quad (A.2)$$

The main assumption in the above formulation of the Maxwell–Stefan equation and the equation for the electrochemical potential of component i is that pressure differences and/or other external forces do not affect the mass transfer process. Besides, it is assumed that the transport process takes place isothermally.

It is preferable to express the driving force of the mass transfer process as a function of one set of variables, namely the mole fractions of the components present in the liquid mixture. The derivation of the transport equations can be split into three parts:

1. Derivation of an expression of the electrical potential gradient as a function of the gradient in the activity.
2. Derivation of an expression of the gradient in the activity as a function of the gradient in the mole fractions.
3. Rearrangement of the set of Maxwell–Stefan equations.

A.2.1. Derivation of an expression of the electrical potential gradient as a function of the gradient in the activity (see also Newman, 1963)

The Maxwell–Stefan equation for component i can be rewritten as[3]:

[2] In the following $\nabla\mu_k$ should be read as $\nabla_{T,P}\mu_k$.

[3] $$\begin{aligned}\Sigma_{j=1}^{n} K_{i,j}(v_j - v_i) &= \Sigma_{j=1}^{n} K_{i,j}(v_j - v_i) - v_n\Sigma_{j=1}^{n} K_{i,j} + v_n\Sigma_{j=1}^{n} K_{i,j}\\ &= \Sigma_{\substack{j=1\\ j\neq i}}^{n} K_{i,j}v_j + K_{i,i}v_i - \Sigma_{j=1}^{n} K_{i,j}v_i\\ &\quad - v_n\Sigma_{\substack{j=1\\ j\neq i}}^{n} K_{i,j} - v_n K_{i,i} + v_n\Sigma_{j=1}^{n} K_{i,j}\\ &= \Sigma_{\substack{j=1\\ j\neq i}}^{n} K_{i,j}(v_j - v_n)\\ &\quad + (K_{i,i} - \Sigma_{j=1}^{n} K_{i,j})(v_i - v_n)\\ &= \Sigma_{j=1}^{n} M_{i,j}(v_j - v_n).\end{aligned}$$

$$c_i\nabla\mu_i = RT\sum_{j=1}^{n}\frac{c_i c_j}{c_T \text{Đ}_{i,j}}(v_j - v_i) = \sum_{j=1}^{n} K_{i,j}(v_j - v_i)$$

$$= \sum_{j=1}^{n} M_{i,j}(v_j - v_n) \quad (A.3)$$

with:

$$M_{i,j} = K_{i,j} \quad i \neq j = 1, 2, \ldots, n \quad (A.3a)$$

$$M_{i,i} = K_{i,i} - \sum_{k=1}^{n} K_{i,k} \quad i = 1, 2, \ldots, n \quad (A.3b)$$

$$K_{i,j} = RT\frac{x_i x_j c_T}{\text{Đ}_{i,j}} \quad (A.3c)$$

The mass transport in a mixture of n components can be described fundamentally with n Maxwell–Stefan equations. However, due to the Gibbs–Duhem relationship only $n-1$ Maxwell–Stefan equations are independent. With this restriction, the preceding Eq. (A.3c) can be rewritten as:

$$v_j - v_n = -\sum_{k=1}^{n-1} L^n_{j,k} c_k \nabla\mu_k \quad (A.4)$$

with:

$$[L^n] = -[M^n]^{-1} \quad (A.4a)$$

$[M^n]$ is obtained from $[M]$ in which the nth row and the nth column has been removed[4].

The current density I can be obtained from the component velocities[5]:

$$I = F\sum_{i=1}^{n} z_i c_i v_i = F\sum_{i=1}^{n-1} z_i c_i v_i + F z_n c_n v_n$$

$$= F\sum_{i=1}^{n-1} z_i c_i v_i - F v_n \sum_{i=1}^{n-1} z_i c_i = F\sum_{i=1}^{n-1} z_i c_i (v_i - v_n)$$

$$= -F\sum_{i=1}^{n-1} z_i c_i \sum_{k=1}^{n-1} L^n_{i,k} c_k \nabla\mu_k$$

$$= -F\sum_{i=1}^{n-1} c_i \nabla\mu_i \sum_{k=1}^{n-1} L^n_{k,i} c_k z_k \quad (A.5)$$

Definition of κ and t_i^n

If no concentration gradients are present in the liquid phase, then the expression for the electrochemical potential gradient reduces to:

$$\nabla\mu_i = z_i F \nabla\varphi \quad (A.6)$$

Substitution of Eq. (A.6) into Eq. (A.5) results in the following relation for I:

$$I = -F^2\nabla\varphi\sum_{i=1}^{n-1} z_i c_i \sum_{k=1}^{n-1} L^n_{i,k} z_k c_k = -\kappa\nabla\varphi \quad (A.7)$$

with:

$$\kappa = c_T^2 F^2 \sum_{i=1}^{n-1}\sum_{j=1}^{n-1} z_i z_j x_i x_j L^n_{i,j} \quad (A.8)$$

In other words, if no concentration-driven mass transfer occurs, then the relationship between the current density and the electrical potential gradient follows Ohm's law (κ is the conductivity of the solution, $1/\kappa$ is a kind of electrical resistance).

The contribution of each component to the current density I can be expressed with the help of a transference number for each component (except the nth). The transference number t_i^n is defined as follows:

$$t_i^n I = -t_i^n \kappa \nabla\varphi = c_i z_i F(v_i - v_n) \Rightarrow t_i^n$$

$$= \frac{z_i x_i c_T^2 F^2}{\kappa}\sum_{k=1}^{n-1} L^n_{i,k} z_k x_k \quad (A.9)$$

N.B.:

$$\sum_{i=1}^{n-1} t_i^n = 1$$

Eq. (A.8) can also be written as:

$$\sum_{k=1}^{n-1} L^n_{i,k} z_k x_k = \frac{t_i^n \kappa}{z_i x_i c_T^2 F^2} \quad (A.10)$$

Introduction of κ and t_i^n in the relation Eq. (A.9)

If concentration gradients are present in the liquid phase (which is the case with membrane processes), then Eq. (A.5) changes after combination with Eq. (A.10) to:

$$I = -F\sum_{i=1}^{n-1} c_i \nabla\mu_i \sum_{k=1}^{n-1} L^n_{k,i} c_k z_k = -\frac{\kappa}{F}\sum_{i=1}^{n-1}\frac{t_i^n}{z_i}\nabla\mu_i \quad (A.11)$$

Substitution of Eq. (A.2) in Eq. (A.11) results into:

$$I = -\frac{\kappa^{n-1}}{F}\sum_{i=1}^{n-1}\frac{t_i^n}{z_i}\{RT\nabla(\ln(x_i\gamma_i)) + z_i F\nabla\varphi\}$$

$$= -\kappa\nabla\varphi - \frac{RT\kappa^{n-1}}{F}\sum_{i=1}^{n-1}\frac{t_i^n}{z_i}\nabla(\ln(x_i\gamma_i)) \quad (A.12)$$

from which the following expression for the electrical potential gradient is obtained:

$$\nabla\varphi = -\frac{I}{\kappa} - \frac{1}{F}\sum_{i=1}^{n-1}\frac{t_i^n}{z_i}\nabla\mu_i^{\text{chemical}}$$

$$= -\frac{I}{\kappa} - \frac{RT}{F}\sum_{i=1}^{n-1}\frac{t_i^n}{z_i}\nabla(\ln(x_i\gamma_i)) \quad (A.13)$$

The first part of the right hand side of Eq. (A.13) gives the Ohmic contribution to the electrical potential, the second part gives the diffusion potential, which is a correction of the electrical potential gradient due to the presence of concentration differences in the solution.

[4] Note that $[M]$, $[M^n]$ and $[L^n]$ are symmetrical.

[5] With the derivation of Eq. (A.5) the condition of electroneutrality has been applied, which can be formulated as follows $\Sigma_{i=1}^{n} z_i x_i = c_T\Sigma_{i=1}^{n} z_i x_i = \Sigma_{i=1}^{n} z_i c_i = 0$.

A.2.2. Derivation of an expression of the gradient in the activity as a function of the gradient in the mole fractions

Rearrangement of the set of Maxwell–Stefan equations.

According to Taylor and Krishna (1993) the following expression can be derived:

$$d_i = \sum_{j=1}^{n-1} \Xi_{i,j} \nabla x_j - \frac{x_i z_i F I}{RT\kappa} = \sum_{j=1}^{n} \frac{x_i N_j - x_j N_i}{c_T Đ_{i,j}} \tag{A.14}$$

As pointed out by Taylor and Krishna (1993), the molar flux N_i needs to be defined with respect to a certain reference frame. For this case, the velocity of the nth component will be chosen as the reference frame in order to obtain the diffusive flux of the other components. For the diffusive flux (J_i^n), which is the flux of component i with respect to the velocity of component n, the following relation can be derived:

$$J_i^n = N_i - c_i v_n \tag{A.15}$$

The diffusive flux J_n^n is equal to zero with this definition (Taylor & Krishna, 1993).

Eq. (A.14) can now be rearranged to (Taylor & Krishna, 1993):

$$d_i = \sum_{j=1}^{n-1} B_{i,j}^n J_j^n \tag{A.16}$$

with:

$$B_{i,i}^n = -\frac{1}{c_T} \sum_{k=1\, i\neq k}^{n} \frac{x_k}{Đ_{i,k}} \quad i = 1, 2, \ldots, n-1 \tag{A.16a}$$

$$B_{i,j}^n = \frac{x_i}{c_T Đ_{i,j}} \quad i \neq j = 1, 2, \ldots, n-1 \tag{A.16b}$$

The set of $n-1$ Maxwell–Stefan equations for the description of the mass transfer in an n-component mixture can be represented in matrix notation as follows:

$$(d) = [\Xi](\nabla x) - (Z) = [B^n](J^n) \tag{A.17}$$

with:

$$Z_i = \frac{x_i z_i F I}{RT\kappa} \quad i = 1, 2, \ldots, n-1 \tag{A.17a}$$

The gradient in the mole fraction follows from Eq. (A.17):

$$[\Xi](\nabla x) = [B^n](J^n) + (Z) \tag{A.18}$$

However, the set of $(n-1)$ equations defined by Eq. (A.18) contains one dependent equation due to the condition of electroneutrality. It is possible to eliminate the dependent equation by substituting the following relations into Eq. (A.18):

$$I = F \sum_{i=1}^{n} z_i N_i = F \sum_{i=1}^{n} z_i J_i^n \tag{A.19}$$

and:

$$\sum_{i=1}^{n} \nabla x_i = 0 \tag{A.20a}$$

$$\sum_{i=1}^{n} z_i \nabla x_i = 0 \tag{A.20b}$$

Rearrangement of Eq. (A.18) with the help of Eqs. (A.19), (A.20a) and (A.20b) yields:

$$[\Xi*](\nabla x) = [B^n*](J^n) + (Z^*)I \tag{A.21}$$

with:

$$\Xi_{i,j}^* = \Xi_{i,j} - \Xi_{i,n-1} \frac{z_j - z_n}{z_{n-1} - z_n} \quad i = 1 \ldots n-2;$$
$$j = 1, \ldots, n-2 \tag{A.22a}$$

$$B_{i,j}^n* = B_{i,j}^n - B_{i,n-1}^n \frac{z_j}{z_{n-1}} \quad i = 1 \ldots n-2;$$
$$j = 1, \ldots, n-2 \tag{A.22b}$$

$$Z_i^* = \left(\frac{x_i z_i F}{RT\kappa} + \frac{B_{i,n-1}^n}{F z_{n-1}} \right) \quad i = 1, \ldots, n-2 \tag{A.22c}$$

Eq. (A.21) can be reworked to:

$$(J^n) = [A](\nabla x) - (\alpha)I \tag{A.22}$$

with:

$$[A] = [B^n*]^{-1}[\Xi*] \tag{A.22a′}$$

$$(\alpha) = [B^n*]^{-1}(Z^*) \tag{A.22b′}$$

This equation can be further rewritten as:

$$(J^n) = [A](\nabla x) - [\beta]x \tag{A.23}$$

with:

$$[\beta] = [B^n*]^{-1}[Z^\#]$$

in which:

$$Z_{i,j}^\# = 0 \quad i \neq j = 1, 2, \ldots, n-2 \tag{A.24.a}$$

$$Z_{i,i}^\# = \left(\frac{z_i F}{RT\kappa} + \frac{1}{F c_T Đ_{i,n-1} z_{n-1}} \right) I \quad i = 1, 2, \ldots, n-2 \tag{A.24.b}$$

Relationship (Eq. (A.23)) defines a set of $n-2$ independent equations, which can be solved with the help of to following supplementary equations:

$$\sum_{i=1}^{n} z_i x_i = 0 \qquad \text{(condition of electroneutrality)}$$

$$\sum_{i=1}^{n} x_i = 1 \tag{A.25}$$

Eq. (A.23) is the basic equation for the description of the mass transport in a electrochemical system. This equation can be further adjusted for the membrane electrolysis process. The membrane in these processes is often modeled as a component, in which the membrane

concentration is chosen equivalent to the concentration of the fixed charged groups in the membrane and the ionic charge of the membrane (z_{membrane}) equivalent to the charge of the charged groups in the membrane. In membrane processes the reference velocity with the application of the Maxwell–Stefan theory is often the velocity of the membrane, which is (mostly) 0 m s^{-1}. If the membrane is the nth component Eq. (A.15) can be written as:

$$v_n = \frac{-1}{c_m} J_m^n = 0 \tag{A.26}$$

If the membrane is the nth component in the system, then the molar flux of component i (for $i = 1, \ldots, n-2$) follows from:

$$N_i = J_i^n - c_i v_n = J_i^n - \frac{c_i}{c_m} J_i^n$$

$$= J_i^n - \frac{x_i}{x_{\text{membrane}}} J_{\text{membrane}}^n = J_i^n \tag{A.27}$$

in which J_i^n follows from Eq. (A.23). If component $(n-1)$ is ionic, the flux of this component can be easily calculated using Eq. (A.19). Otherwise, for component $(n-1)$ it is also possible to calculate the flux by substituting the resulting calculated mole fraction profile in Eq. (A.23). With the known mole fraction profile, the potential profile can now be calculated using Eq. (A.13).

A.3. Final model equations

In conclusion this gives for the present system.

- $n-2$ Independent Maxwell–Stefan equations for components 1–$n-2$:

  $$(N) = [A](\nabla x) - [\beta]x \tag{A.28}$$

  in which N is the matrix with the $(n-2)$ fluxes with respect to the (in time and space stationary) membrane.
- Two supplementary equations for component $n-1$ and n:

  $$\sum_{i=1}^{n} z_i x_i = 0 \quad i = n-1 \tag{A.29}$$

  $$\sum_{i=1}^{n} x_i = 1 \quad i = n \tag{A.30}$$

  in which matrix A contains diffusivities, thermodynamic non-idealities and transference numbers:

  $$[A] = [B^n{*}]^{-1}[\Xi{*}] \tag{A.31}$$

The matrix $[A]$ can be divided into two parts:

- One matrix with diffusivities $[B^n{*}]$.
- One matrix with thermodynamic non-idealities and transference numbers $[\Xi{*}]$; and matrix β with diffusivities and the current density:

$$[\beta] = [B^n{*}]^{-1}[Z^{\#}] \tag{A.32}$$

The different matrices are defined as.

- Matrix with diffusivities $[B^n{*}]$:

  $$B_{i,j}^n{*} = B_{i,j}^n - B_{i,n-1}^n \frac{z_j}{z_{n-1}} \quad i = 1, \ldots, n-2 \tag{A.33}$$

  with:

  $$B_{i,i}^n = -\frac{1}{c_{\text{T}}} \sum_{k=1 k \neq i}^{n} \frac{x_k}{Đ_{i,k}} \tag{A.33a}$$

  $$B_{i,j}^n = \frac{x_i}{c_{\text{T}} Đ_{i,j}} \quad i \neq j \tag{A.33b}$$

- Matrix with thermodynamic non-idealities and transference numbers $[\Xi]$:

  $$\Xi_{ij}^{*} = \Xi_{i,j} - \Xi_{i,n-1} \frac{z_j - z_n}{z_{n-1} - z_n} \quad i = 1, \ldots, n-2$$

  $$j = 1, \ldots, n-2 \tag{A.34}$$

  with:

  $$\Xi_{i,j} = \Gamma_{i,j} - x_i z_i \sum_{k=1}^{n-1} \Gamma_{k,j} \frac{t_k^n}{z_k x_k} \tag{A.34a}$$

  $$\Gamma_{i,j} = \delta_{i,j} + x_i \left.\frac{\partial \ln \gamma_i}{\partial x_j}\right|_{T,P,x_k,k \neq j = 1 \ldots n-1} \tag{A.34b}$$

  $$t_j^n = \frac{z_j x_j c_{\text{T}}^2 F^2}{\kappa} \sum_{k=1}^{n-1} L_{j,k}^n z_k x_k \tag{A.34c}$$

  $$\kappa = c_{\text{T}}^2 F^2 \sum_{i=1}^{n-1} \sum_{j=1}^{n-1} z_i z_j x_i x_j L_{i,j}^n \tag{A.34d}$$

  $$[L^n] = -[M^n]^{-1} \tag{A.34e}$$

  $[M^n]$ follows from $[M]$ in which the nth row and column have been removed:

  $$M_{i,j} = K_{i,j} \quad i \neq j = 1, 2, \ldots, n \tag{A.34f}$$

  $$M_{i,i} = K_{i,i} - \sum_{k=1}^{n} K_{i,k} \quad i = 1, 2, \ldots, n \tag{A.34g}$$

  $$K_{i,j} = RT \frac{x_i x_j c_{\text{T}}}{Đ_{i,j}} \tag{A.34h}$$

- Matrix with diffusivities and current density $Z^{\#}$:

  $$Z_{i,j}^{\#} = 0 \quad i \neq j = 1, 2, \ldots, n-2 \tag{A.35a}$$

  $$Z_{i,i}^{\#} = \left(\frac{z_i F}{RT\kappa} + \frac{1}{F c_{\text{T}} Đ_{i,n-1} z_{n-1}}\right) I \quad i = 1, 2, \ldots, n-2 \tag{A.35b}$$

References

Mason, E. A., & Malinauskas, A. P. (1983). *Gas Transport in Porous Media*: *The Dusty Gas Model*, *Chemical Engineering Monographs*, vol. 17. Amsterdam: Elsevier.

Newman, J. S. (1963). *Electrochemical Systems*. Englewoods Cliffs, NJ: Prentice-Hall.

van der Stegen, J. H. G., van der Veen, A. J., Weerdenburg, H., Hogendoorn, J. A., & Versteeg, G. F. (1999a). Application of the Pitzer model for the estimation of activity coefficients of electrolytes in ion selective membranes. *Fluid Phase Equilibria*, *157*, 181–196.

van der Stegen, J. H. G., van der Veen, A. J., Weerdenburg, H., Hogendoorn, J. A., & Versteeg, G. F. (1999b). Application of the Maxwell–Stefan theory to the transport in ion-selective membranes used in the chloralkali electrolysis process. *Chemical Engineering Science*, *54*, 2501–2511.

Taylor, R., & Krishna, R. (1993). *Multicomponent Mass Transfer*. New York: Wiley.

Taylor, R., Hoefsloot, H. C. J., & Kuipers, J. A. M. (1995). Reader of the course. In *Numerical Method for Chemical Engineers*. The Netherlands: Enschede.